



## Understanding the real behavior of Mote and 802.11 ad hoc networks: an experimental approach

Giuseppe Anastasi<sup>a,b</sup>, Eleonora Borgia<sup>a,c</sup>, Marco Conti<sup>a,c,\*</sup>,  
Enrico Gregori<sup>a,c</sup>, Andrea Passarella<sup>a,b</sup>

<sup>a</sup>*Pervasive Computing & Networking Laboratory (PerLab)*

<sup>b</sup>*Department of Information Engineering, University of Pisa, Via Diotisalvi, 2 – 56122 Pisa, Italy*

<sup>c</sup>*IIT Institute, National Research Council (CNR), Via G. Moruzzi, 1 – 56124 Pisa, Italy*

Accepted 2 March 2005

Available online 23 March 2005

---

### Abstract

IEEE 802.11 and Mote devices are today two of the most interesting wireless technologies for ad hoc and sensor networks respectively, and many efforts are currently devoted to understanding their potentialities. Unfortunately, few works adopt an experimental approach, though several papers highlight that popular simulation and analytical approximations may lead to very inaccurate results. In this paper we discuss outcomes from an extensive measurement study focused on these technologies. We analyze the dependence of the communication range on several parameters, such as node distance from the ground, transmission data rate, environment humidity. Then, we study the extent of the physical carrier sensing zone around a sending node. On the basis of these elements, we provide a unified wireless link model for both technologies. Finally, by using this model we analyze well-known scenarios (such as the hidden node problem), and we modify the traditional formulations according to our experimental results.

© 2005 Elsevier B.V. All rights reserved.

*Keywords:* 802.11; Mica Motes; Ad hoc networks; Sensor networks; Experimental measurements

---

\* Corresponding author at: IIT Institute, National Research Council (CNR), Via G. Moruzzi, 1 – 56124 Pisa, Italy. Tel.: +39 050 315 3062; fax: +39 050 315 2593.

*E-mail addresses:* [g.anastasi@iet.unipi.it](mailto:g.anastasi@iet.unipi.it) (G. Anastasi), [e.borgia@iit.cnr.it](mailto:e.borgia@iit.cnr.it) (E. Borgia), [m.conti@iit.cnr.it](mailto:m.conti@iit.cnr.it) (M. Conti), [e.gregori@iit.cnr.it](mailto:e.gregori@iit.cnr.it) (E. Gregori), [a.passarella@iet.unipi.it](mailto:a.passarella@iet.unipi.it) (A. Passarella).

## 1. Introduction

Self-organizing wireless networks are nowadays one of the hottest topics in the area of pervasive computing. The research community is devoting a lot of effort to designing protocols to support Mark Weiser's pervasive networking vision. Mostly, 802.11-based ad hoc networks and sensor networks are being investigated. While 802.11-based devices have emerged as the de-facto standard technology for investigating ad hoc networks, no counterparts exist on the sensor-networks side. The most widespread devices are Berkeley Motes [15] that are thus assumed as the reference sensor-network technology also in this paper.

The vast majority of works on wireless networks rely on simulation models for evaluations, the main reason being the ease of development and reproducibility with respect to real experiments. However, relying just on simulations may be misleading. Specifically, it is well known that accurately modeling the signal propagation on a wireless medium is a hard task. Unfortunately, an accurate model is often required to correctly evaluate the effectiveness of higher-layer protocols. For example, [10,18] show that the performances of routing protocols (e.g., AODV, DSR) highly depend on the physical-layer model used in simulations. In some cases, simulation results are extremely different from experimental measurements. Furthermore, the relative comparison among couples of protocols can be completely swapped by changing the physical-layer model. These observations remind us that simulation models and outcomes should be *validated against experimental measurements*.

These remarks are the main motivation for the work presented in this paper. Specifically, we report the main results from a wide measurement study focused on 802.11 and Mote wireless networks. The emphasis of the paper is on characterizing key networking features such as the maximum communication distance<sup>1</sup> between a couple of nodes, and the interactions between concurrent transmitting nodes. We study the effect on the communication distance of several environmental parameters (e.g., humidity, distance from the ground), providing quantitative evidence of their impact. For example, the communication distance of Mote nodes on foggy days can drop to one fifth of the communication distance on dry days. We also account for the effect of technology-dependent parameters, such as the bit rate, and the antenna directionality. We find that the communication distance of 802.11 nodes significantly varies with the data rate, and we sketch possible side effects on routing protocols. We also find that Mote antennas are strongly directional, and nodes need to be very carefully placed in order to communicate.

Then, we study the effect of concurrent transmitters on each other. Since both technologies adopt a CSMA/CA MAC protocol, the Physical Carrier Sensing mechanism determines the interaction between concurrent senders. Our measures show that for both technologies, Physical Carrier Sensing – and, thus, the dependence among couples of transmitters – extends far beyond the maximum communication distance. Roughly, the

---

<sup>1</sup> As discussed in the paper, the wireless channel for both technologies is not isotropic. Therefore, we prefer referring to the distance at which two nodes can communicate as the communication *distance* instead of the communication *range*.

maximum Physical Carrier Sensing distance is (at least) twice as large as the maximum communication distance.

On the basis of these measurements we provide a channel model for both 802.11 and Mote devices. It is worth noting that, while the numerical values (e.g., the maximum communication distance) depend on the particular technology, the *structures* of the channels are very similar in the two cases. Therefore, the two channel models can be seen as particular instances of a *unified* channel model. This is very important, since the same channel model can be used to analyze both 802.11 and Mote networks, just by tuning the model parameters.

Finally, we exploit the channel model definition to elaborate on the well-known hidden and exposed node problems. The formulations currently reported in computer networking handbooks do not take into consideration the effect of Physical Carrier Sensing beyond the communication distance. Due to the large extension of Physical Carrier Sensing, we find that these formulations should be significantly revised. Hence, we provide novel formulations, which comply with the measurement outcomes.

The rest of the paper is organized as follows. [Section 2](#) describes the experimental methodology we have adopted, and provides some background on the 802.11 and Mote technologies. [Section 3](#) analyzes the bandwidth available at the application level for both technologies. This analysis is exploited to understand the networking features under investigation. [Section 4](#) is devoted to characterizing the maximum distance at which a couple of nodes can correctly communicate. [Section 5](#) presents the results related to Physical Carrier Sensing, and defines the channel model for 802.11 and Mote nodes. Finally, [Section 6](#) surveys works related to ours, while [Section 7](#) highlights the lessons learned from our measurement study.

## 2. Methodology

### 2.1. Experiment test-bed

The 802.11 measurement test-bed is based on laptops running the Linux-Mandrake 8.2 operating system and equipped with D-LinkAir DWL-650 cards using the DSSS physical layer operating at the nominal bit rates of 1, 2, 5.5 and 11 Mbps. They communicate in the ISM band, at 2.4 GHz. The components of the 802.11 test-bed are very common commercial devices, and do not require further description. On the other hand, it is interesting to focus more carefully on the Mote test-bed, since this technology is relatively new. Berkeley Motes come in two different sensor nodes, *Mica2* and *Mica2dot*, that have similar characteristics but a different form factor. *Mica2* are  $58 \times 32 \times 7$  mm shaped, while *Mica2dot* are  $25 \times 7$  mm (coin-size) shaped. Both *Mica2* and *Mica2dot* sensor nodes have an 8-bit Atmel microprocessor (running at 8 MHz and 4 MHz, respectively). They are shipped with 128 kB of program memory, 4 kB of RAM, and 512 kB of non-volatile flash memory that can be used for logging and data collection. For wireless communication, Motes use an RFM ChipCon radio that provides a nominal bit rate of 19.2 kbps. Specifically, they communicate in the ISM band, at 868/916 MHz. Motes are powered by the TinyOS operating system that is specifically tailored to such devices [8].

---

```

1  Initial_backoff = rand(15ms,68.3ms);
2  sMacDelay=Initial_backoff;
3  Start Timer(sMacDelay);
4  Repeat {
5      Upon timer expiration do {
6          if(not (received_preamble() and busy_channel()))
7              then {
8                  transmit the frame;
9                  exit();
10             }
11             else {
12                 congestion_backoff=rand(12.08ms,193.3ms);
13                 sMacdelay=Congestion_backoff;
14                 Start Timer(sMacDelay);
15             }
16         }
17     }
18 forever;

```

---

Fig. 1. Pseudo-code of the Mote MAC protocol.

Both technologies use a CSMA/CA MAC protocol to communicate. Familiarity with the protocols' mechanisms is required to understand our measurement results. Therefore, we briefly survey the MAC protocols used by both 802.11 and Mote networks. The MAC protocol adopted by Mica Motes is based on CSMA/CA. This protocol works as follows (see Fig. 1). Upon receiving a frame to transmit, the sensor node generates a random *Initial\_backoff* interval, uniformly distributed in the range [15, 68.3] ms, and starts a timer (lines 1–3). Then, it enters a loop in which it performs the following actions (lines 4–18). Upon timer expiration the channel is sensed. If it is found idle and no incoming frame is detected the frame is transmitted (lines 4–10). On the hand, if the channel is found busy the sensor node generates a further random time interval (*congestion\_backoff*), uniformly distributed in the range [12.08, 193.3] ms, and starts the backoff timer again (lines 11–14). The above actions are repeated until the channel is found free and the frame is thus transmitted. Please note that this MAC protocol does not include any mechanism for detecting failed transmissions (e.g., ACK frames as in the IEEE 802.11). Thus, higher-level protocols are in charge of detecting collisions and frame corruptions. Furthermore, Motes do not continuously sense the channel during backoff intervals. This is a power-saving measure, as it gives the opportunity to switch-off the radio subsystem during such time intervals.

Since many detailed descriptions of the 802.11 MAC protocol are available in the literature (see for example [3]), we here just sketch its main functionalities. The MAC protocol of 802.11 networks is based on CSMA/CA as well, but includes several additional functionalities with respect to the Motes' protocol. Specifically, frames are explicitly acknowledged, thus making it possible to detect collisions and frame corruptions directly

at the MAC layer. The congestion avoidance scheme is based on backoff intervals as well. However, backoff intervals are uniformly distributed in a range that increases exponentially after each unsuccessful attempt. Furthermore, the channel is continuously sensed during backoff intervals, and the backoff procedure is frozen when other stations' transmissions are detected. Different types of frame have different transmit priorities. Frame fragmentation and a Power-Saving Mode are also included in the MAC protocol definition.

As claimed in [Section 1](#), the target of our study is understanding key communication features of 802.11 and Mote devices. Therefore in our experiments we consider static, single-hop scenarios, i.e., communicating stations are within their transmission range and stations do not change their position during the experiment. This allows us to remove other possible factors that may interfere with the target of the experiments, e.g., link breakage, route re-computation. The detailed definition of each experiment setup (i.e., number of devices, placement, hardware configuration, etc.) is provided throughout the paper. All the experiments we present here are performed in outdoor space, i.e., a field without buildings. We do not report results from indoor experiments, since these results are strongly affected by the effect of signal reflections, and are thus dependent on the particular indoor environment.

## 2.2. *Experiment plan*

The first feature we hereafter characterize is the maximum available bandwidth, i.e., the maximum throughput that can be achieved at the application level between a sending and a receiving node. The goal of this set of experiments is twofold. On one hand, they allow us to understand which fraction of the raw data rate is available at the application level, and hence they measure the overhead introduced by lower-level protocols. On the other hand, since they measure the maximum application-level throughput, they represent a reference point for other results presented in the paper, mainly those related to the Carrier-Sensing characterization (see [Section 5.1](#)).

The next topic that we address is deriving an experiment-based channel model for 802.11 and Mote networks. To this end, since both technologies utilize CSMA MAC protocols, two main features have to be characterized, i.e., the communication distance and the Carrier-Sensing zone. As far as the communication distance, we measure the maximum distance at which a receiving node is able to correctly detect transmissions of a sending node. We use the packet reception probability as the main performance figure for this set of experiments. Specifically, we define the maximum communication distance as the point where the packet reception probability drops below 85%. Also in this case, we run a first set of measurements with an optimal configuration to achieve a reference point. Afterward, we replicate the experiments to evaluate the effect of single parameters on the communication distance. Specifically, we show the effect on the communication distance of physical data rate, environment humidity, device height from the ground, and antennae orientation. To the best of our knowledge, the effect of several of these parameters on the communication distance has never been highlighted before. In the last experiments, we measure the Carrier-Sensing zone. As explained in detail in [Section 5.1](#), the technique used

Table 1  
Maximum throughput derived from the analytical model

802.11			Motes	
Data rate	$m = 512$ B	$m = 1024$ B	Data rate	$m = 36$ B
11 Mbps	3.337 Mbps	5.120 Mbps	19.2 kbps	4.43 kbps
5.5 Mbps	2.490 Mbps	3.428 Mbps		
2 Mbps	1.319 Mbps	1.589 Mbps		
1 Mbps	0.758 Mbps	0.862 Mbps		

to measure the Carrier-Sensing zone relies on the throughput measurements presented in the first part of the paper.

As a final remark, it is worth noting that all experiments have been replicated several times to increase results reliability. The results that we present are the average values over the different replicas.

### 3. Available bandwidth

In this section we analyze the maximum throughput offered by the MAC protocol of 802.11 and Mote devices to upper layers. This is performed through an analytical model validated against experiment outcomes. Due to the lack of space, we only provide the model results. More details can be found in [4,8]. Table 1 reports the values derived from the model by varying some key parameters of the test-bed. Specifically, we consider three typical values for the application-level packet size, i.e. 512 B and 1024 B for 802.11 applications, and 36 B for Motes applications. For the 802.11 technology, we also consider the possible data rates (the Motes technology defines a single data rate, 19.2 kbps). The model can be used to derive the throughput also for other parameter values (e.g., for different packet sizes), since its results closely match experiment outcomes [4,8].

The most interesting issue is that just a small percentage of the theoretical data rate is available as application-level throughput. As expected, this percentage increases with the payload size. However, in the case of 802.11 networks, even with large packet sizes (e.g.,  $m = 1024$  B) the bandwidth utilization is in the order of 46%. It is also worth noting that the higher the data rate, the lower the benefit of further increases of the data rate. Specifically, doubling the data rate from 1 Mbps to 2 Mbps results in throughput increase in the order of 80%. Doubling the data rate from 5.5 Mbps to 11 Mbps results in throughput increase around 40%. This feature stems from backward compatibility issues of 802.11 devices. To assure interoperability between legacy 802.11 (operating at 1 Mbps and 2 Mbps) and 802.11b nodes (operating also at 5.5 Mbps and 11 Mbps), different portions of a frame are transmitted at different data rates. Higher data rates (e.g., 11 Mbps) are used to transmit just the MAC-layer payload; thus the overhead of MAC- and physical-layer headers increases as the (payload) data rate increases.

The high impact of MAC-level mechanisms on the throughput is even more evident in the case of Motes devices. In this case the bandwidth utilization is in the order of

23%. Moreover, this value is achieved for the maximum MAC-layer payload size (i.e.,  $m = 36$  B), and hence it represents an upper bound. However, it should be noted that MAC protocols for sensor networks are designed to be energy efficient, rather than to assure high application-level throughput. For typical sensor-network applications, a few kbps can be sufficient.

#### 4. Communication distance

The goal of this section is to characterize the “communication zone” of a sending node S, meaning the zone around S where other nodes can receive S’s transmissions. Mostly, we are interested in understanding what the maximum communication distance at which a receiver can correctly receive S transmissions is.

Several works in the literature highlight that the shape of the communication zone greatly depends on the environment where nodes are placed [1,2,4,10,16,22,23]. To have a reference point, we firstly try to avoid measurements biasing by environment parameters. To this end, we collect a first set of measures by using a couple of nodes – say S and R – where S is the sender and R the receiver. S and R communicate in open space to avoid the influence of obstacles. Experiments are run on sunny days, as humidity has a great impact on the communication distance (see below). In addition, nodes are placed high enough to avoid signal reflections on the ground and antennas are oriented so as to maximize their performance in connecting S and R. We place S and R at a variable distance from each other, and we measure the probability of R correctly receiving a packet sent by S.

##### 4.1. Impact of communication distance on Micas’ packet receptions in an optimal environment

Fig. 2 shows the packet reception probability as a function of the distance between S and R for Motes devices. Specifically, Fig. 2(a) refers to Mica2 nodes, while Fig. 2(b) refers to Mica2dot nodes. Recall that we define the maximum communication distance as the point where the packet reception probability drops below 85%. In the former case, the maximum communication distance is around 55 m, while in the latter case it rises up to 135 m.<sup>2</sup> This is a very interesting result, as it shows that: (i) Mote devices can support quite long communication distances, and (ii) Mica2dot technology significantly outperforms Mica2 technology.

The improvement in the hardware technology between Mica2 and Mica2dot emerges from a second feature of Fig. 2, as well. Specifically, Mica2 nodes show a quite irregular behavior immediately beyond the maximum communication distance. Note that between 55 m and 65 m the packet reception probability has a large variance (i.e., the minimum, average and maximum values collected during the experiments are quite different), and increasing the distance may result in higher packet reception probability. This behavior has been previously observed [1,9,16,22,13], and is usually referred to as the “gray-zone phenomenon”. There exists a gray zone (beyond the maximum communication distance)

---

<sup>2</sup> Please note that the transmission power was set to the default value, i.e., 0 dBm.

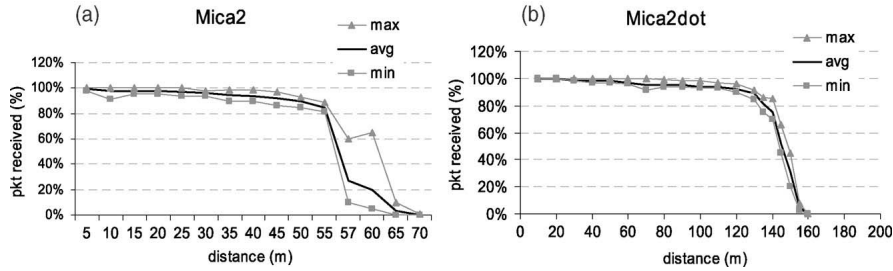


Fig. 2. Packet reception probability for Mica2 (a) and Mica2dot (b).

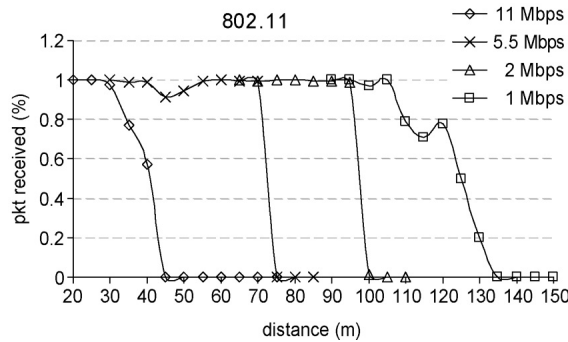


Fig. 3. Packet reception probability for 802.11 nodes.

in which the packet reception probability is very unstable and quite random. The packet reception probability can show non-monotonic decrease within this region (i.e., nodes farther away from the sender can see a better link than nodes closer to the sender). Moreover, the size of this zone is not negligible (in our experiments it is about 10 m). The node behavior in the gray zone depends on many parameters, one of the most important being the quality of the receiver circuitry. If we focus on Fig. 2(b), we can see that the gray-zone phenomenon is far less evident. Specifically, the gray zone size is always large, since the packet reception probability drops to 0 just around 150 m. But the packet reception probability is far more stable with respect to the Mica2 case. As “external” factors (such as obstacles) are avoided in this setup, we believe that the different behavior stems from the improved quality of the Mica2dot receiver.

#### 4.2. Impact of communication distance on 802.11 nodes’ packet reception in an optimal environment

We replicate similar experiments by using 802.11 nodes as well, and we plot the outcomes in Fig. 3. In this case, we derive a different curve for each of the data rates defined in the 802.11b standard [12], i.e., 1 Mbps, 2 Mbps, 5.5 Mbps and 11 Mbps. Results plotted in Fig. 3 are interesting in many respects. Specifically:

- (i) some gray-zone phenomena can be observed also in this case, mainly at 1 Mbps data rate;
- (ii) the maximum communication distance is larger for lower data rates; this is intuitive, since at low data rates more energy is packed with each bit transmitted, and hence transmissions can travel farther away;
- (iii) the maximum communication distance changes significantly with the data rate; specifically, it is around 30 m at 11 Mbps, 70 m at 5.5 Mbps, 90–100 m at 2 Mbps and 110–130 m at 1 Mbps.

Point (iii) above has two very important consequences. First of all, it is interesting to compare the communication distance used in the most popular simulation tools, like ns-2 and Glomosim/Qualnet, with the outcomes of our experiments. In these simulation tools a communication distance equal to 250 m and 376 m is assumed, respectively. Since the above simulation tools typically consider a 2 Mbps bit rate we refer to the communication distance estimated for the 2 Mbps data rate. As is clear, the value used in the simulation tools (and, hence, in the simulation studies based on them) is 2–3 times higher than the values measured in practice. This difference is very important for example when studying the behavior of routing protocols: the shorter the communication distance, the higher the frequency of route re-calculation when the network nodes are mobile. Clearly, the maximum communication distance depends on the transmission power. Our results are obtained by setting the transmission power to 15 dBm.

The large difference of communication distances at different data rates has another important side effect. It is worth recalling that, to allow interoperability with legacy 802.11 nodes, different MAC-level frames are transmitted at different rates by 802.11b nodes. For example, control frames such as RTS, CTS and ACK are typically transmitted at 1 or 2 Mbps, irrespective of the data rate used to transmit data frames. Therefore, assuming that the RTS/CTS mechanism is active, if a node transmits a data frame at 11 Mbps to another node within its transmission range (i.e., less than 30 m apart) it reserves the channel for a radius of approximately 90 (120) m around itself. Such behaviors may severely impact routing-protocols performance, as shown in [14].

#### *4.3. Impact of communication distance in a non-optimal environment*

The setup of the experiments presented so far is quite optimistic, since it limits as much as possible factors that may reduce the signal propagation such as obstacles and humidity. In this section we show how much the maximum communication distance is affected by two environment parameters, i.e., the humidity, and the nodes' height from the ground. In these experiments, the other test-bed parameters are as in the optimal configuration.

##### *4.3.1. Humidity*

Fig. 4 highlights the influence of humidity on the communication distance. Specifically, Fig. 4(a) shows the difference between the packet reception probability experienced by 802.11 nodes transmitting at 1 Mbps on a sunny and a cloudy day, respectively. Fig. 4(b) plots the packet reception probability experienced by Mica2 nodes in the presence of fog and rain. The packet reception probability on dry days (derived from Fig. 2(a)) is also plotted for comparison. From Fig. 4 it clearly emerges that humidity plays a

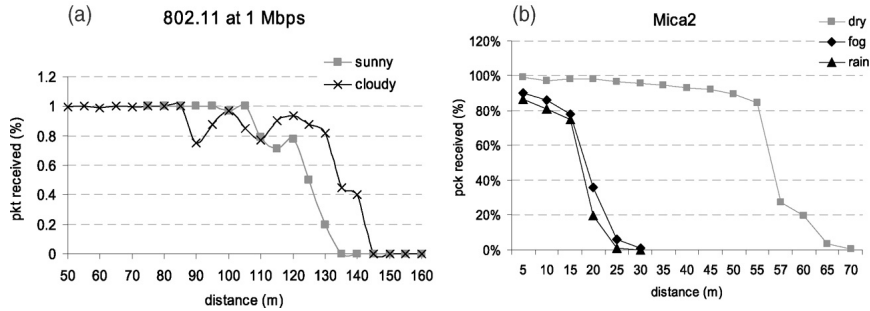


Fig. 4. Communication distance in humid environments for 802.11 (a) and Motes (b) devices.

substantial role in determining nodes' communication distances. The decrease of the communication distance in humid environments is caused by water particles that interact with electromagnetic waves and absorb part of their energy causing signal attenuation. Of course, the absorption and signal-attenuation magnitude depend on the waves' frequency, and are hence different for 802.11 and Motes technologies.<sup>3</sup> It is particularly interesting observing the plot in Fig. 4(b). The communication distance drops from 55 m to 10 m moving from dry to humid environments. This observation is very important, since sensor networks could be deployed to run unattended in outdoor environments, where humidity can actually be an important issue (see, for example, the Great Duck Island Project [17]).

#### 4.3.2. Height from the ground

While running the experiments presented so far, we observed a dependence of the communication distance on the mobile devices' height from the ground. Specifically, in some cases we observed that, while the nodes were not able to communicate when located on stools, they started to exchange packets on lifting them up. In the rest of this section we present the results obtained by a careful investigation of this phenomenon. Specifically, we study the dependence of the communication distance on the devices' height from the ground.

Fig. 5(a) plots the packet reception probability as a function of the nodes' height from the ground, in the case of 802.11 nodes. In particular, the measures are collected by placing the nodes, S and R, 30 m apart, and by setting the data rate to 11 Mbps (similar results have also been observed for different data rates [4]). Fig. 5(b) is the analogous plot with respect to Mote devices. In this case, S and R are placed 10 m apart. From results presented in Figs. 2 and 3, S and R are within the corresponding maximum communication distance in both cases. Therefore, the packet reception probability should be close to 100%. In contrast, Fig. 5 shows that the communication distance depends on the nodes' height from the ground, and is reduced when the nodes' height is low.

<sup>3</sup> Recall that in our setup 802.11 nodes communicate in the 2.4 GHz band, while Motes communicate in the 868/916 MHz band.

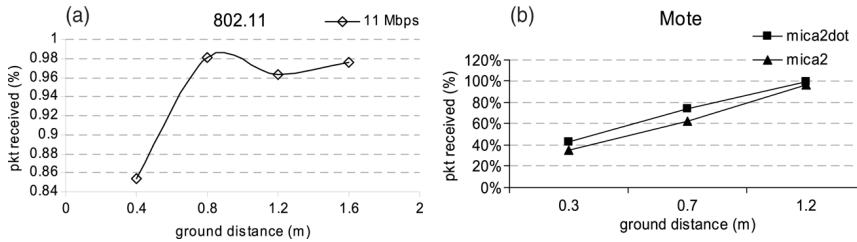


Fig. 5. Impact of node height on the communication distance for 802.11 (a) and Motes (b) devices.

The work presented in [11] provides a theoretical framework for explaining this phenomenon. Due to lack of space, we here omit describing this framework, and just report the analytical results. More complete discussions can be found in [2,4]. The analytical model predicts that – in our test-bed configuration – effects related to ground reflections disappear if the distance from the ground of 802.11 (Mote) nodes is greater than 0.97 m (0.93 m). Results from this analytical framework are thus aligned with our measurements.

#### 4.4. Hardware configuration impact

To complete the discussion about the communication distance, we show that also the particular configuration of nodes' hardware has a big impact. Specifically, in this section we highlight the dependence of the communication distance on the antenna orientation. The dependence on the transmission power has also been investigated. Due to lack of space, we omit these results, which can be found in [8]. Also for this set of experiments, the other test-bed parameters are as in the optimal configuration. The focus of this section is mainly on Mote nodes. Similar phenomena, sometime less marked, occur in the case of 802.11 nodes as well.

In early stages of measurements with Mote devices we noted that the nodes' antennas need to be placed very carefully in order for nodes to communicate. This behavior suggests that antennas shipped with Motes have very directional beams, and motivates us to better understand the dependence of communication distance on antenna orientation. Therefore, we replicate the experiments by varying the relative angle between the sender and receiver antennas. For example, Fig. 6 shows the two extreme cases for Mica2 and Mica2dot nodes. The two curves refer to the case when the angle between the antennas is equal to 0 and  $\pi/2$ , respectively. Fig. 6 confirms our preliminary observation about the strong directionality of Motes' antennas. We believe this could be a big problem for real sensor network applications, where it might be practically unfeasible to precisely control the nodes' placement.

## 5. Channel model

In the previous section we have analyzed the networking features of 802.11 and Mote devices in terms of communication distance. This analysis is not sufficient for deriving the

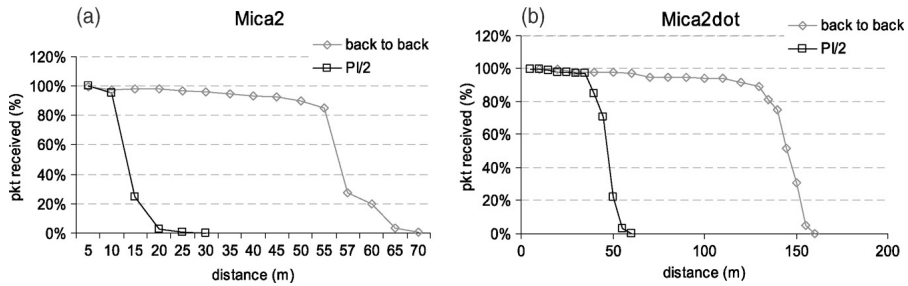


Fig. 6. Communication distance as a function of antenna orientation for Mica2 (a) and Mica2dot (b).

channel models for the reference technologies. The wireless medium has neither absolute nor readily observable boundaries outside of which nodes are known to be unable to sense a signal. Therefore, due to the carrier sensing nature of the MAC protocols used by both technologies, couples of nodes may interact also at a distance far greater than the maximum communication distance. The goal of this section is hence to characterize node interactions due to Carrier Sensing, and eventually to provide a channel model for both 802.11 and Mote technologies.

### 5.1. Physical Carrier Sensing

In this section we investigate the extent of the Physical Carrier Sensing zone, i.e., we measure the maximum distance at which a node N2 senses the channel busy due to an ongoing transmission of a node N1. A direct measure of this quantity seems difficult to achieve because neither with 802.11 nor with Mote devices is it possible to have information about the channel carrier sensing. Therefore, we define an indirect way to perform these measurements. We utilize the scenario shown in Fig. 7. Nodes A and C are sending, while nodes B and D are receiving. The distance in sender–receiver couples is fixed ( $d(A, B) = d(C, D) = 10$  m), while the distance between the two couples (i.e.,  $d(B, C)$ ) is variable. All the other test-bed parameters are as in the optimal configuration. We increase  $d(B, C)$  until no correlation is measured between the couples of nodes. To quantify the degree of correlation between the two sessions we measure (at the application level) the throughput of each session in isolation, i.e., when the other session is not active. Then we measure the throughput achieved by each session when both sessions are active. Obviously, no correlation exists when the aggregate throughput is equal to the sum of the throughputs of the two sessions in isolation.

Figs. 8 and 9 show the results from our measurements. Specifically, the aggregated throughput experienced by the two sessions in isolation, and while concurrently running, is plotted. To show that, as expected, the Carrier Sensing is independent of the data rate, we replicate the 802.11 experiments by setting the data rate at 11 Mbps (Fig. 8(a)) and 2 Mbps (Fig. 8(b)), respectively. In the case of Mote devices, we use Mica2dot nodes (Fig. 9). As clearly appears from Fig. 8, there are two steps in the 802.11 aggregate throughput: one after 180 m and the other after 250 m. This behavior can be explained as follows. Taking a session as a reference, the presence of the other session may have two possible

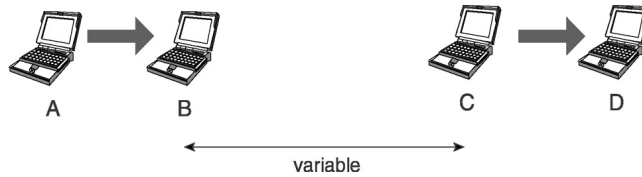


Fig. 7. Setup used to measure the Physical Carrier Sensing zone.

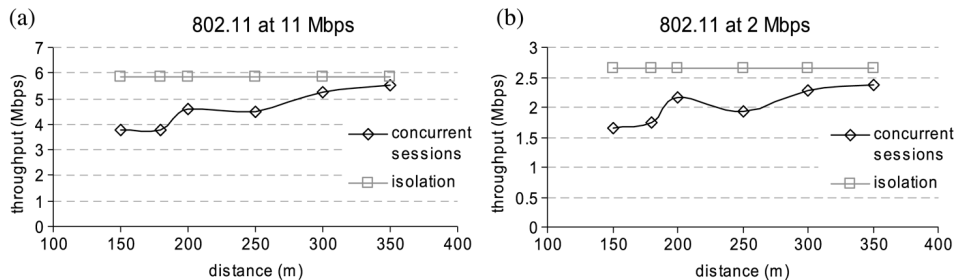


Fig. 8. Sessions' throughput for 802.11 devices at 11 Mbps (a) and 2 Mbps (b).

effects on the performance of the reference session: (1) if the two sessions are within the same Physical Carrier Sensing zone, they share the same physical channel; (2) if they are outside of each other's Physical Carrier Sensing zones, the radiated energy from one session may still affect the quality of the channel observed by the other session. As the radiated energy may extend over unlimited distances, we can expect the second effect to completely disappear only for very large distances among the sessions [7]. Hence, we can assume that the first step in Fig. 8(a) and (b) coincides with the end of the Physical Carrier Sensing zone, while the second one occurs when even the second effect becomes almost negligible. It is worth noting that the extent of the Physical Carrier Sensing zone is almost the same for the two different transmission rates. The Physical Carrier Sensing mainly depends on two parameters: the nodes' transmitting power and the distance between transmitting nodes. The rate at which data are transmitted has no effect on these parameters.

A very interesting analogy can be observed by comparing Figs. 8 and 9. Specifically, the throughput pattern in Fig. 9 presents the same two steps highlighted for 802.11 nodes. In the case of Mica2dot nodes, the limit of the Physical Carrier Sensing zone can be set at 275 m, while the two sessions are completely independent at 450 m.

On the basis of the above results, two very interesting outcomes can be drawn:

- 802.11 and Mote technologies show very similar qualitative behaviors as regards carrier sensing;
- in both cases, the Physical Carrier Sensing zone extends at least twice as much as the communication zone.

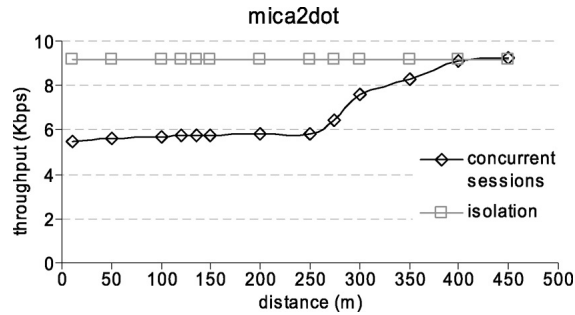


Fig. 9. Sessions' throughput for Mica2dot Mote devices.

## 5.2. Unified channel model

The results shown in Sections 4 and 5.1 allow us to derive a very interesting analogy between the channel structures observed in 802.11 and Mote networks. Both technologies present a zone around the sender where the packet reception probability is high and pretty stable. Beyond the maximum communication distance, a gray zone exists, where the packet reception probability drops towards 0 in a somewhat random way. Finally, a pretty large zone exists where the packet reception probability is 0, but carrier sensing is active. Based on these remarks it is possible to define a *unified* channel model for both technologies. Fig. 10 gives a pictorial representation of this model. Specifically, given a transmitting node S as reference,

- nodes within the communication zone are able to correctly receive transmissions from S;
- nodes beyond the communication zone but within the gray zone *may* correctly receive transmissions from S; nodes close to each other in this region may experience completely different qualities of the link with S;
- nodes beyond the gray zone but within the Physical Carrier Sensing zone cannot correctly receive transmissions from S; however, when S is transmitting they observe the channel busy and thus they defer their transmissions;
- nodes beyond the Physical Carrier Sensing zone do not measure any significant energy on the channel when S is transmitting; therefore they can start transmitting contemporarily to S; however, the quality of the channel they observe may be affected by the energy radiated by S.

It should be noted that this is just a *qualitative* representation. The actual shape and extent of the different zones depend on the particular technology, and on the environment nodes are operating in. The results presented in Sections 4 and 5.1 show how different parameters impact this channel model with respect to each technology. In particular, we have shown that:

- data rate has an important effect on the 802.11 nodes' communication zone;
- fog/rain may significantly reduce the communication zone extent for Mote nodes;

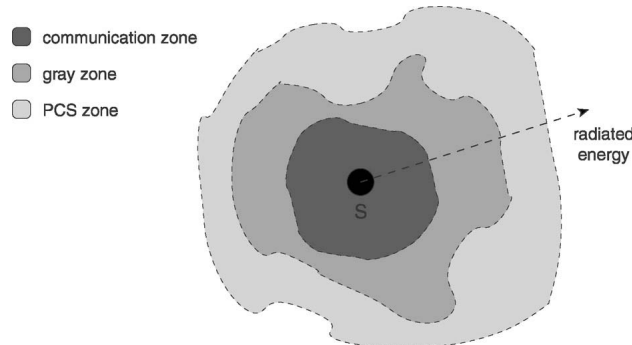


Fig. 10. Unified channel model.

- the shape of the communication zone is far from circular for Mote nodes due to strong antenna directionality;
- the packet reception probability within the gray zone is more regular for Mica2dot and 802.11 nodes than for Mica2 nodes;
- the size of the Physical Carrier Sensing zone does not depend on the data rate; this means that, according to our measurements, 802.11 nodes operating at 11 Mbps block concurrent transmissions in a zone six times larger than the communication zone.

Despite the quantitative difference between the two technologies, envisioning a unified channel model is very important. For example, just a single model needs to be deployed in network simulators. Then, model parameters can be set so as to represent the particular technology under investigation. Since correctly modeling the physical channel feature is a hard task, this may save significant effort.

Adopting our experiment-based channel model leads to very interesting remarks. For example, once this channel model is assumed, the traditional formulations of the hidden and exposed node problems do not hold any longer. For the sake of space, we here briefly discuss the case of the hidden node problem. The interested reader is referred to [4] for more details. The hidden node problem is usually presented as in Fig. 11(a), where circles denote the communication ranges.<sup>4</sup> Node A (C) is hidden to node C (A), since it is outside C's (A's) communication range. Therefore A and C can transmit at the same time, thus colliding at node B.

On comparing Fig. 11(a) with Fig. 10 it is clear that these formulations do not hold in practice. In the case of Fig. 11(a), nodes A and C will be in each other's Physical Carrier Sensing ranges. Therefore, they will sense their respective ongoing transmissions, thus avoiding collisions at node B. Furthermore, using RTS/CTS mechanisms (as proposed in 802.11 networks [12]) achieves the same goal of Physical Carrier Sensing (but introduces an additional overhead), while it does not help at all in the case of exposed nodes (see [4]).

<sup>4</sup> For ease of reading, in the following we assume that zones of the channel model have a perfect circular shape. Extending the analysis to more general cases is straightforward.

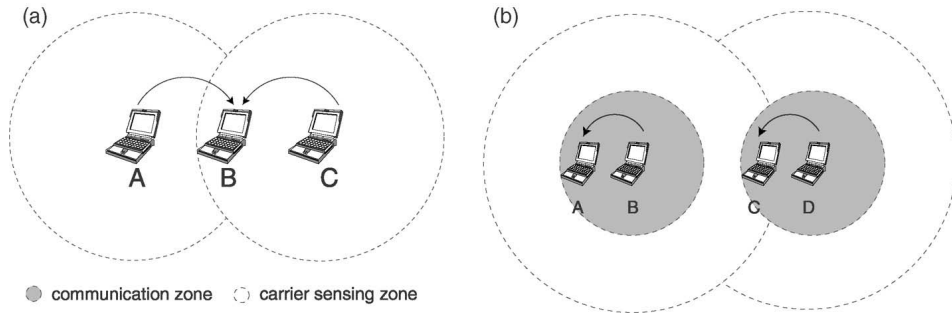


Fig. 11. Traditional and novel formulations of the hidden node problem.

The channel model described in this section leads to new formulations of the hidden and exposed node problems. Let us focus on Fig. 11(b). In this figure we have two transmitting nodes, B and D, that are outside their respective Physical Carrier Sensing ranges and, hence, are hidden from each other. In addition, we assume that the receiver of node D (denoted by C in the figure) is inside the Physical Carrier Sensing range of node B. In this scenario B and D can transmit simultaneously. If the noise experienced by C, as a side effect of B's transmission, is strong enough, C cannot correctly detect D's transmissions. It is worth noting that RTS/CTS mechanisms do not help solving this problem, and new coordination mechanisms need to be designed. Extending the coordination in the channel access beyond the Physical Carrier Sensing zone seems to be the correct direction for solving the above problems. This may be achieved by cross-layer interactions among a link-state routing protocol and the MAC layer. For example, periodic link-state advertisements sent by C might be exploited to spread information about the channel load C is experiencing. The MAC layer of B and D may use this information to tune the CSMA algorithm. The interested reader is referred to [6] for details.

## 6. Related works

Currently, the relevance of wireless ad hoc networks experimental studies is growing, as witnessed by the increasing number of papers focusing on either 802.11 or Mote technologies. The importance of an experimental approach in evaluating wireless networks is discussed also in [10,14,18]. The present work stems from the 802.11 experimental analyses presented in [4,5], and from the Mote experimental analyses presented in [2, 8]. Starting from these results, this work highlights analogous features among 802.11 and Mote nodes. Such analogies highlight that the *structures* of the wireless channels are very similar in the two cases. Thus, it is possible to define a unified channel model that encompasses both technologies. To the best of our knowledge, this is the first work that highlights such analogies, and provides a unified channel model.

Other works in the literature utilize measurements to characterize 802.11 communication features. Ref. [1] studies the link properties of an 802.11 mesh network, and finds quite large gray zones where the packet reception probability is very unstable.

The reference network is deployed in a urban environment, and this has an important influence on the results. Refs. [10,13] report measurements from a large 802.11 ad hoc test-bed, deployed in open space. Ref. [13] highlights that the quality of wireless links strongly depend on several environment parameters, and this results in asymmetric links, non-isotropic communication zones and large gray zones. Finally, [13] highlights that common modeling assumptions used in simulations do not hold in reality, resulting in quite unreliable results. A similar conclusion is also drawn in [10]. Starting from real measurements, this work shows that the comparison among routing protocols can be completely inverted by adopting commonly used modeling assumptions. In our experiments, we have found some of the wireless link features highlighted in [1,10,13], as well. In addition, we have provided new results, such as the impact of humidity on the maximum communication distance. Moreover, in this paper we have also measured the extent of the Physical Carrier Sensing zone, which, obviously, has a big impact on the performance of CSMA/CA-based MAC protocols.

Experimental studies have been done also with respect to Mote sensor networks. A very detailed characterization of wireless link features is provided by [22]. This work shows how obstacles in the environment affect the packet reception probability. Furthermore, pretty large gray zones are found in any setup (i.e., both outdoor and indoor). The existence of gray zones is also highlighted in [16]. In addition, this work provides a detailed characterization of the effects of antenna directionality. The observation of similar features is the starting point of [9,19,23]. In particular, [19] focuses on the effect of link asymmetry and gray zones on routing protocols. Ref. [9] shows that these wireless link features can impact not only the routing layer, but also the MAC and application level. Finally, [23] proposes a new physical-layer model for complying with wireless link irregularity (e.g., asymmetric links), and – by using this model – analyzes the performance of different MAC and routing protocols.

As compared with [9,19,23], our work is more focused on characterizing the wireless link characteristics, and is thus closer to [16,22]. With respect to these papers, we have provided novel results, such as the influence of humidity and ground distance. Furthermore, our work is the only one that studies the Physical Carrier Sensing zone of Mote nodes.

The impact of Physical Carrier Sensing on ad hoc networks has been studied in [20,21]. Ref. [20] highlights that, to prevent the hidden node problem, Physical Carrier Sensing is as effective as the RTS/CTS mechanism, provided that the carrier sensing range is at least twice as large as the communication range. In this case, the RTS/CTS mechanism is just an overhead. While [20] relies just on simulation and analysis, in this paper we have verified this point through real experiments. Furthermore, through our experiments we have also analyzed the exposed node problem, and we have provided new formulations of both problems, according to the experiment outcomes.<sup>5</sup> Finally, [21] studies the joint effect of data rate, Physical Carrier Sensing and network density on the aggregated throughput achieved in ad hoc networks. By means of analytical models and simulation, [21] shows that, at the optimal operating point of the network, the carrier sensing range is around twice

---

<sup>5</sup> The redefinition of the exposed node problem has not been included in this work, for space reasons. It can be found in [4].

as large as the maximum communication range. This is actually the same property that we have highlighted for 802.11 nodes operating at 1 Mbps, and for Mica Motes. In particular, our results show that 802.11 (Mote) networks achieve the maximum aggregated throughput for network densities such that the optimal data rate is 1 Mbps (19.2 kbps).

## 7. Conclusions

In this paper we have characterized several key networking features of 802.11 and Mote devices. We have adopted an experimental approach, since real measurements are strongly required to understand the actual behavior of wireless networks. The choice of focusing on 802.11 and Mote nodes relies on the fact that they are the two most commonly used technologies for ad hoc and sensor networks, respectively. The experimental results presented in this paper have confirmed that basing wireless network models on experiments, and validating simulation outcomes against experimental results, is necessary for deriving reliable conclusions about wireless network behavior.

First of all, we analyzed the maximum communication distance, i.e., the maximum distance at which two nodes are able to correctly detect transmissions of each other. This part of the analysis has shown that several assumptions that are commonly used in simulation and analytical models should be carefully revised. For example, the dependence of the communication distance on the physical data rate is typically not modeled in 802.11 simulations. Furthermore, common simulation models assume communication distances far greater than what we measured in reality. Among other effects, this may lead to unreliable evaluations of routing protocol performances. The impact of environment parameters should be carefully modeled as well, mainly in sensor networks. For example, parameters such as height from the ground and humidity have to be taken into consideration to provide realistic models of sensor networks for environmental applications.

A second set of experiments has been devoted to analyze the Physical Carrier Sensing zone, i.e., the zone around a sending node within which another node senses the channel busy. Interestingly, we have found that this zone is at least twice as large as the communication zone. On the basis of these measurements, we have defined a wireless link model for 802.11 and Mote devices. We have highlighted that the behavior of the wireless link is very similar in both cases. Therefore, it is possible defining a unified wireless link model that encompasses both technologies. The results presented in the former part of the paper allow us to define a particular instance of the model, with respect to each specific technology.

The model we have derived from experimental results is quite different from traditional wireless network models. Specifically, no sharp boundary exists between the region (around a sending node) where packets can be correctly received, and the region where packets are not received at all. Instead, a pretty large “gray zone” exists, where the packet reception probability is almost unpredictable. Finally, a large Carrier-Sensing zone extends outside the gray zone. Experiments have also shown that the shape of these zones (i.e., the communication zone, the gray zone, and the Carrier-Sensing zone) is not a perfect sphere around the sender, but is quite irregular, and depends on several environment and node-configuration parameters. We believe that using such a realistic channel model in

simulation and analytical evaluations is key to clearly understanding wireless network performances. For example, the traditional hidden and exposed node formulations has to be revised once our model is assumed.

## Acknowledgements

This work was partially funded by the Italian Ministry for Education, University and Scientific Research (MIUR) under the FIRB-VICOM and FIRB-PERF projects, and by the Information Society Technologies Programme of the European Commission, Future and Emerging Technologies, under the IST-2001-38113 MOBILEMAN project.

## References

- [1] D. Aguayo, J. Bicket, S. Biswas, G. Judd, R. Morris, Link-level measurements from an 802.11b mesh network, in: Proc. of SIGCOMM 2004, August 30–September 3, Portland, OR, 2004.
- [2] G. Anastasi, M. Conti, E. Gregori, A. Falchi, A. Passarella, Performance measurements of mote sensor networks, in: Proceedings of the ACM/IEEE International Symposium on Modeling, Analysis and Simulation of Wireless and Mobile System, 4–6 October, Venice, Italy, 2004.
- [3] G. Anastasi, M. Conti, E. Gregori, IEEE 802.11 ad hoc networks: protocols, performance and open issues, in: S. Basagni, M. Conti, S. Giordano, I. Stojmenovic (Eds.), *Ad Hoc Networking*, IEEE Press and John Wiley and Sons, Inc., New York, 2004.
- [4] G. Anastasi, E. Borgia, M. Conti, E. Gregori, Wi-Fi in ad hoc mode: a measurement study, in: Proceedings of the IEEE International Conference on Pervasive Computing and Communications, PerCom 2004, 14–17 March, Orlando, FL, 2004.
- [5] G. Anastasi, E. Borgia, M. Conti, E. Gregori, IEEE 802.11 ad hoc networks: performance measurements, in: Proc. of the Workshop on Mobile Wireless Networks (MWN 2003), Co-located with IEEE ICDCS 2003, May 22, Providence, RI, 2003.
- [6] E. Borgia et al., MobileMAN Project Deliverable D10, Architecture, Protocols and Services, October 2004, Available at <http://cnd.iit.cnr.it/mobileMAN/deliverables/IST-2001-38113MOBILEMAN-D10.pdf>.
- [7] T. Ephremides, A wireless link perspective in mobile networking, in: ACM Mobicom 2002 Keynote Speech, Available at <http://www.acm.org/sigmobile/mobicom/2002/program/>.
- [8] A. Falchi, Sensor networks: performance measurements with motes technology, Laurea Thesis, University of Pisa, Italy, 2004, Available at <http://etd.adm.unipi.it/theses/available/etd-05252004-154652/>.
- [9] D. Ganesan, D. Estrin, A. Woo, D. Culler, B. Krishnamachari, S. Wicker, Complex behavior at scale: an experimental study of low-power wireless sensor networks, Tech. Rep. UCLA/CSD-TR 02-0013, Computer Science Department, UCLA, July 2002.
- [10] R. Gray, D. Kotz, C. Newport, N. Dubrovsky, A. Fiske, J. Liu, C. Masone, S. McGrath, Outdoor experimental comparison of four ad hoc routing algorithms, in: Proceedings of the ACM/IEEE International Symposium on Modeling, Analysis and Simulation of Wireless and Mobile System, 4–6 October, Venice, Italy, 2004.
- [11] D.B. Green, M.S. Obaidat, An accurate line of sight propagation performance model for ad hoc 802.11 wireless LAN (WLAN) devices, in: Proceedings of IEEE ICC 2002, New York, April 2002.
- [12] IEEE Standard 802.11, Wireless LAN Medium Access Control (MAC) and Physical Layer (PHY) Specifications, August 1999.
- [13] D. Kotz, C. Newport, R. Gray, J. Liu, Y. Yuan, C. Elliot, Experimental evaluation of wireless simulation assumptions, in: Proceedings of the ACM/IEEE International Symposium on Modeling, Analysis and Simulation of Wireless and Mobile System, 4–6 October, Venice, Italy, 2004.
- [14] H. Lundgren, E. Nordström, C. Tschudin, The gray zone problem in IEEE 802.11b based ad hoc networks, *ACM SIGMOBILE Mobile Computing and Communications Review* 6 (3) (2002).
- [15] Mica2 and Mica2Dot Datasheets, Available at <http://www.xbow.com/>.

- [16] N. Reijers, G. Halkes, K. Langendoen, Link layer measurements in sensor networks, in: Proc. of the First IEEE International Conference on Mobile Ad hoc and Sensor Systems, MASS 2004, 24–27 October, Fort Lauderdale, FL, 2004.
- [17] R. Szcwcyk, J. Polastre, A. Mainwaring, D. Culler, Lessons from a sensor network expedition, in: Proc. of the First European Workshop on Wireless Sensor Networks, EWSN'04, January 2004.
- [18] M. Takai, J. Martin, R. Bagrodia, Effects of wireless physical layer modeling in mobile ad hoc networks, in: Proceedings of the 2001 ACM International Symposium on Mobile Ad Hoc Networking & Computing, MobiHoc 2001, October 2001, pp. 87–94.
- [19] A. Woo, T. Tong, D. Culler, Taming the underlying challenges of reliable multihop routing in sensor networks, in: Proc. of The First ACM Conference on Embedded Networked Sensor Systems, SenSys 2003, 5–7 November, Los Angeles, CA, 2003.
- [20] K. Xu, M. Gerla, S. Bae, How effective is the IEEE 802.11 RTS/CTS handshake in ad hoc networks?, in: Proc. of the IEEE Global Communications Conference, GLOBECOM 2002, 17–27 November, Taipei, Taiwan, 2002.
- [21] X. Yang, N.H. Vaidya, On the physical carrier sense in wireless ad hoc networks, in: Proc. of the Annual Joint Conference of the IEEE Computer and Communications Societies, INFOCOM 2005, 13–17 March, Miami, FL, 2005.
- [22] J. Zhao, R. Govindan, Understanding packet delivery performance in dense wireless sensor networks, in: Proc. of The First ACM Conference on Embedded Networked Sensor Systems, SenSys 2003, 5–7 November, Los Angeles, CA, 2003.
- [23] G. Zhou, T. He, S. Krishnamurthy, J.A. Stankovic, Impact of radio irregularity on wireless sensor networks, in: Proc. of the Second International Conference on Mobile Systems, Applications, and Services, MobiSys 2004, 6–9 June, Boston, MA, 2004.